Broadband optical transparency in plasmonic nanocomposite polymer films via exciton-plasmon energy transfer

R. Dhama,[1] A. R. Rashed,[2,3] V. Caligiuri,[1] M. El. Kabbash,[2] G. Strangi,[1,2] and A. De Luca[1,*]

[1]*Department of Physics and CNR - Nanotec, University of Calabria, 87036 Rende, Italy*
[2]*Department of Physics, Case Western Reserve University, 44106-7079 Cleveland, USA*
[3]*Nanotechnology Research Center, Bilkent University, 06800 Ankara, Turkey*
[*]*antonio.deluca@fis.unical.it*

Abstract: Inherent absorptive losses affect the performance of all plasmonic devices, limiting their fascinating applications in the visible range. Here, we report on the enhanced optical transparency obtained as a result of the broadband mitigation of optical losses in nanocomposite polymeric films, embedding core-shell quantum dots (CdSe@ZnS QDs) and gold nanoparticles (Au-NPs). Exciton-plasmon coupling enables non-radiative energy transfer processes from QDs to metal NPs, resulting in gain induced transparency of the hybrid flexible systems. Experimental evidences, such as fluorescence quenching and modifications of fluorescence lifetimes confirm the presence of this strong coupling between plexcitonic elements. Measures performed by means of an ultra-fast broadband pump-probe setup demonstrate loss compensation of gold NPs dispersed in plastic network in presence of gain. Furthermore, we compare two films containing different concentrations of gold NPs and same amount of QDs, to investigate the role of acceptor concentration (Au-NPs) in order to promote an effective and efficient energy transfer mechanism. Gain induced transparency in bulk systems represents a promising path towards the realization of loss compensated plasmonic devices.

OCIS codes: (260.2160) Energy transfer; (160.4670) Optical materials; (160.5470) Polymers; (320.7100) Ultrafast measurements.

References and links

1. A. Manjavacas, F. J. G. d. Abajo, and P. Nordlander, "Quantum plexcitonics: Strongly interacting plasmons and excitons," Nano Lett. **11**, 2318–2323 (2011).
2. H. Chen, L. Shao, K. C. Woo, J. Wang, and H.-Q. Lin, "Plasmonic-molecular resonance coupling: Plasmonic splitting versus energy transfer," J. Phys. Chem. C **116**, 14088–14095 (2012).
3. M. A. Noginov, G. Zhu, A. M. Belgrave, R. Bakker, V. M. Shalaev, E. E. Narimanov, S. Stout, E. Herz, T. Suteewong, and U. Wiesner, "Demonstration of a spaser-based nanolaser," Nature **460**, 1110–1113 (2009).
4. R. F. Oulton, V. J. Sorger, T. Zentgraf, R. Ma, C. Gladden, L. Dai, G. Bartal, and X. Zhang, "Plasmon lasers at deep subwavelength scale," Nature **461**, 629–632 (2009).
5. A. O. Govorov, G. W. Bryant, W. Zhang, T. Skeini, J. Lee, N. A. Kotov, J. M. Slocik, and R. R. Naik, "Exciton-plasmon interaction and hybrid excitons in semiconductor-metal nanoparticle assemblies," Nano Lett. **6**, 984–994 (2006).
6. J. N. Anker, W. P. Hall, O. Lyandres, N. C. Shah, J. Zhao, and R. P. Van Duyne, "Biosensing with plasmonic nanosensors," Nat. Mater. **7**, 442–453 (2008).

#261630 Received 22 Mar 2016; revised 9 May 2016; accepted 9 May 2016; published 21 Jun 2016

7. S. A. Maier, "Plasmonic field enhancement and SERS in the effective mode volume picture," Opt. Express **14**, 1957–1964 (2006).
8. J. B. Pendry, "Negative refraction makes a perfect lens," Phys. Rev. Lett. **85**, 3966–3969 (2000).
9. X. Zhang and Z. Liu, "Superlenses to overcome the diffraction limit," Nat. Mater. **7**, 435–441 (2008).
10. S. Ishii, V. M. Shalaev, and A. V. Kildishev, "Holey-metal lenses: Sieving single modes with proper phases," Nano Lett. **13**, 159–163 (2013).
11. R. J. Thompson, G. Rempe, and H. J. Kimble, "Observation of normal-mode splitting for an atom in an optical cavity," Phys. Rev. Lett. **68**, 1132–1135 (1992).
12. T. Yoshie, A. Scherer, J. Hendrickson, G. Khitrova, H. M. Gibbs, G. Rupper, C. Ell, O. B. Shchekin, and D. G. Deppe, "Vacuum rabi splitting with a single quantum dot in a photonic crystal nanocavity," Nature **432**, 200–203 (2004).
13. T. Aoki, B. Dayan, E. Wilcut, W. P. Bowen, A. S. Parkins, T. J. Kippenberg, K. J. Vahala, and H. J. Kimble, "Observation of strong coupling between one atom and a monolithic microresonator," Nature **443**, 671–674 (2006).
14. E. Cohen-Hoshen, G. W. Bryant, I. Pinkas, J. Sperling, and I. Bar-Joseph, "Exciton-plasmon interactions in quantum dot-gold nanoparticle structures," Nano Lett. **12**, 4260–4264 (2012).
15. D. Ratchford, F. Shafiei, S. Kim, S. K. Gray, and X. Li, "Manipulating coupling between a single semiconductor quantum dot and single gold nanoparticle," Nano Lett. **11**, 1049–1054 (2011).
16. J. N. Farahani, D. W. Pohl, H.-J. Eisler, and B. Hecht, "Single quantum dot coupled to a scanning optical antenna: A tunable superemitter," Phys. Rev. Lett. **95**, 017402 (2005).
17. A. Balazs, T. Emrick, and T. Russell, "Nanoparticle polymer composites: where two small worlds meet," Science **314**, 1107 (2006).
18. Q. Wang and D. Seo, "Preparation of photostable quantum dot-polystyrene microbeads through covalent organosilane coupling of CdSe@Zns quantum dots," J. Mater. Sci. **44**, 816–820 (2009).
19. I. Pastoriza-Santos, J. Pérez-Juste, G. Kickelbick, and L. M. Liz-Marzán, "Optically active polydimethylsiloxane elastomer films through doping with gold nanoparticles," J. Nanosci. Nanotechnol. **6**, 414–420 (2006).
20. Y. Liu and X. Zhang, "Metamaterials: A new frontier of science and technology," Chem. Soc. Rev. **40**, 2494–2507 (2011).
21. A. Moores and F. Goettmann, "The plasmon band in noble metal nanoparticles: An introduction to theory and applications," New J. Chem. **30**, 1121–1132 (2006).
22. C. M. Soukoulis and M. Wegener, "Optical metamaterials - more bulky and less lossy," Science **330**, 1633–1634 (2010).
23. O. Hess, J. B. Pendry, S. A. Maier, R. F. Oulton, J. M. Hamm, and K. L. Tsakmakidis, "Active nanoplasmonic metamaterials," Nat. Mater. **11**, 573–584 (2012).
24. M. I. Stockman, "Spaser action loss compensation and stability in plasmonic systems with gain," Phys. Rev. Lett. **106**, 156802–1–4 (2011).
25. A. De Luca, M. P. Grzelczak, I. Pastoriza-Santos, L. M. Liz-Marzán, M. L. Deda, M. Striccoli, and G. Strangi, "Dispersed and encapsulated gain medium in plasmonic nanoparticles: A multipronged approach to mitigate optical losses," ACS Nano **5**, 5823–5829 (2011).
26. A. De Luca, M. Ferrie, S. Ravaine, M. La Deda, M. Infusino, A. Rahimi Rashed, A. Veltri, A. Aradian, N. Scaramuzza, and G. Strangi, "Gain functionalized core-shell nanoparticles: The way to selectively compensate absorptive losses," J. Mater. Chem. **22**, 8846–8852 (2012).
27. A. De Luca, R. Dhama, A. R. Rashed, C. Coutant, S. Ravaine, P. Barois, M. Infusino, and G. Strangi, "Double strong exciton-plasmon coupling in gold nanoshells infiltrated with fluorophores," Appl. Phys. Lett. **104**, 103103 (2014).
28. M. Infusino, A. De Luca, A. Veltri, C. Vázquez-Vázquez, M. A. Correa-Duarte, R. Dhama, and G. Strangi, "Loss-mitigated collective resonances in gain-assisted plasmonic mesocapsules," ACS Photonics **1**, 371–376 (2014).
29. G. Strangi, A. De Luca, S. Ravaine, M. Ferrie, and R. Bartolino, "Gain induced optical transparency in metamaterials," Appl. Phys. Lett. **98**, 251912 (2011).
30. H. Hiramatsu and F. E. Osterloh, "A simple large-scale synthesis of nearly monodisperse gold and silver nanoparticles with adjustable sizes and with exchangeable surfactants," Chem. Mater. **16**, 2509–2511 (2004).
31. L. Qu and X. Peng, "Control of photoluminescence properties of CdSe nanocrystals in growth," J. Am. Chem. Soc. **124**, 2049 (2002).
32. S. Shojaei-Zadeh, J. F. Morris, A. Couzis, and C. Maldarelli, "Highly crosslinked poly (dimethylsiloxane) microbeads with uniformly dispersed quantum dot nanocrystals," J. Colloid Interface Sci. **363**, 25 (2011).
33. J. Weaver, R. Zakeri, S. Aouadi, and P. Kohli, "Synthesis and characterization of quantum dot-polymer composites," J. Mater. Chem. **19**, 3198–3206 (2009).
34. D. Uhlenhaut, P. Smith, and W. Caseri, "Color switching in gold-polysiloxane elastomeric nanocomposites," Adv. Mater. **18**, 1653–1656 (2006).
35. A. De Luca, N. Depalo, E. Fanizza, M. Striccoli, M. L. Curri, M. Infusino, A. R. Rashed, M. L. Deda, and G. Strangi, "Plasmon mediated super-absorber flexible nanocomposite for metamaterials," Nanoscale **5**, 6097

#261630 Received 22 Mar 2016; revised 9 May 2016; accepted 9 May 2016; published 21 Jun 2016

(2013).
36. V. Chegel, O. Rachkov, A. Lopatynskyi, S. Ishihara, I. Yanchuk, Y. Nemoto, J. P. Hill, and K. Ariga, "Gold nanoparticles aggregation: Drastic effect of cooperative functionalities in a single molecular conjugate," J. Phys. Chem. C. **116**, 2683–2690 (2012).
37. A. Albanese and W. C. Chan, "Effect of gold nanoparticle aggregation on cell uptake and toxicity," ACS Nano **5**, 5478–5489 (2011).
38. B. Peng, Q. Zhang, X. Liu, Y. Ji, H. Demir, C. H. A. Huan, T. C. Sum, and Q. Xiong, "Fluorophore-doped core-multishell spherical plasmonic nanocavities: Resonant energy transfer toward a loss compensation," ACS Nano **6 (7)**, 6250–6259 (2012).
39. N. Reitinger, A. Hohenau, S. Köstler, J. R. Krenn, and A. Leitner, "Radiationless energy transfer in CdSe/ZnS quantum dot aggregates embedded in PMMA," Phys. Status Solidi A-Appl. Res. **208**, 710–714 (2011).
40. V. N. Pustovit and T. V. Shahbazyan, "Cooperative emission of light by an ensemble of dipoles near a metal nanoparticle: The plasmonic dicke effect," Phys. Rev. Lett. **102**, 077401 (2009).
41. H. N. S. Krishnamoorthy, Z. Jacob, E. Narimanov, I. Kretzschmar, and V. M. Menon, "Topological transitions in metamaterials," Science **336**, 205–209 (2012).
42. K. V. Sreekanth, A. De Luca, and G. Strangi, "Experimental demonstration of surface and bulk plasmon polaritons in hypergratings," Sci Rep **3**, 3291 (2013).
43. S. Xiao, V. P. Drachev, A. V. Kildishev, X. Ni, U. K. Chettiar, H.-K. Yuan, and V. M. Shalaev, "Loss-free and active optical negative-index metamaterials," Nature **466**, 735–738 (2010).

1. Introduction

Nanoplasmonics enables attractive optical properties and various interdisciplinary applications based on localized surface plasmon resonances (LSPRs), defined as resonant collective free electrons oscillations of metallic nanostructures with incident electromagnetic waves. Interaction of LSPs and optical gain such as organic chromophores or quantum dots (QDS), has been a subject of intense research in the last decade, both theoretically and experimentally [1–5]. Exciton-plasmon hybrid systems unearth various promising applications in light harvesting, sensing, plasmon mediated superluminescence, surface enhanced Raman scattering and sub-wavelength imaging beating the diffraction limit [6–10]. Moreover, such systems are also expected to promote quantum effects such as electromagnetically induced transparency, cavity quantum electrodynamics, and photon blockade at normal experimental conditions such as room temperature and atmospheric pressure [11–13]. Several approaches have been implemented in order to study exciton-plasmon interaction, such as using DNA as spacer [14] and placing QDs in close proximity of NPs by using an atomic force microscope (AFM) tip [15,16]. To exploit exciton-plasmon interaction towards real applications, lots of efforts have been made to disperse QDs and plasmonic NPs in polymer matrices [17–19].

However, it is well known that negative real permittivity, an essential condition for realization of metamaterials is always accompanied with a large positive value of imaginary permittivity which diminishes figure of merit FOM = $\mathrm{Re}[\varepsilon(\omega)]/\mathrm{Im}[\varepsilon(\omega)]$ and leads to strong absorptive losses in the plasmonic systems, making plasmonic devices inefficient in the optical range and impossible to harness most of their fascinating properties for real life applications [20, 21]. Battling these absorptive losses will trace the future of nanophotonics and metamaterials. In this context, theoretical and experimental studies suggest that bringing gain close to plasmonic nanostructures can be a potential solution to solve this challenging issue [3, 22–24]. In our former studies, we have successfully demonstrated various loss compensated systems in solutions at nano- and meso-scales, including both gain-functionalized (dye encapsulated into silica shell) and gain assisted (dye dispersed in solution of metal NPs) plasmonic structures [25–29]. However, the evaporation of host solvents can alter gain concentration around plasmonic elements as well as overall concentrations of the systems, affecting the plexcitonic coupling and eventually the loss compensation mechanism. Thus, gain-plasmon interaction must be investigated in a solid, chemically inert and optical transparent host in order to design low loss plasmonic devices and to envisage novel technological ideas.

#261630 Received 22 Mar 2016; revised 9 May 2016; accepted 9 May 2016; published 21 Jun 2016

Here we report on the strong exciton-plasmon coupling between QDs and Au-NPs dispersed in a thick and flexible plastic matrix in order to ensure the host's chemical and physical stability and to prevent change of hybrid system concentration. This particular coupling is responsible for a non-radiative energy transfer from gain medium to the quasi static electric field of the plasmonic elements, through an Exciton-Plasmon Resonance Energy Transfer (EPRET) process, resulting in a modification of the overall absorption and a gain-induced transparency of the plexcitonic systems. Two hybrid nanocomposite films, containing the same concentration of QDs with two different concentrations of Au NPs are also investigated and compared. We confirm that higher concentration of Au NPs leads to comparative proximal neighboring and optimal ratio (critical value of gain around plasmonic NPs) between excitons and plasmons, triggering more efficient non radiative channels via stronger coupling. It has been corroborated by fluorescence quenching, shortening of QDs lifetimes using time correlated single photon counting (TCSPC) data and comparison of threshold values and net enhancement of transmitted probe beam in ultrafast broadband pump-probe experiments in both plexcitonic polymeric films.

2. Methods

Hybrid nanocomposite polymer films are fabricated by starting from the synthesis of Oleylamine (OA-) coated Au-NPs and CdSe@ZnS QDs of 11 nm and 3 nm in diameter, respectively, following the methods reported in references [30, 31]. Dispersion of freshly synthesized OA-capped NPs in a Polydimethylsiloxane (PDMS) matrix resulted in a homogeneous, transparent and free standing thick film containing Au-NPs. On the contrary, when colloidal emitting CdSe@ZnS QDs were added into PDMS pre-polymer mixture, crosslinking of elastomer was not observed in the final films. Absence of crosslinking did not allow PDMS films to be free standing, homogeneous and transparent, even after a long thermal treatment. To overcome this hurdle, change in the QDs surface chemistry presented a promising solution to obtain the desired crosslinking mechanism [32]. OA-capped QDs were successfully incorporated into the PDMS host by playing with nanocrystal surface chemistry, without changing the pre-polymer mixture composition or processing temperature, resulting in effective cross-linked and stable PDMS orange films [32–35].

Six PDMS based nanocomposites samples are synthesized to study the interaction between QDs and Au-NPs in a plastic host matrix. Four samples are used as reference samples (A-B-C-D), while the hybrid nanocomposite films E and F represent the main samples as shown in Fig. 1. Sample A is simply a PDMS matrix, used to study the physical properties of pure polymer network. The second and third samples B and C contain Au-NPs in the plastic host with two different concentrations (B = 1×10^{-6} M and C = 3×10^{-6} M). Sample D was obtained by dispersing CdSe@ZnS QDs (6×10^{-5} M) in the PDMS matrix. The main samples (E and F) contain mixture of similar concentration of QDs and gold NPs at two different concentrations present in samples B and C, respectively. Figure 1 shows the plasmon bands of sample E (brown circles) and sample F (black squares) along with the fluorescence emission of QDs in sample F (red line) with the images of realized systems. Red shift and broadening of plasmon band is due to the presence of a uniform distribution of NP aggregates in the plasmonic polymer films, as well evidenced by optical microscope image reported in Fig.1 (C-50x) [36, 37]. Moreover, uniform distribution of both Au NPs and QDs aggregates of different size in main samples (E and F) is also ensured by the microscope images shown in Fig. 1 (E-50x and F-50x). As QDs emission in samples E and F is quite similar, we reported here only the behavior of sample F in order to exhibit good spectral overlapping with NPs plasmon bands, necessary condition for enabling energy transfer processes via plexcitonic coupling in the two hybrid films.

#261630 Received 22 Mar 2016; revised 9 May 2016; accepted 9 May 2016; published 21 Jun 2016

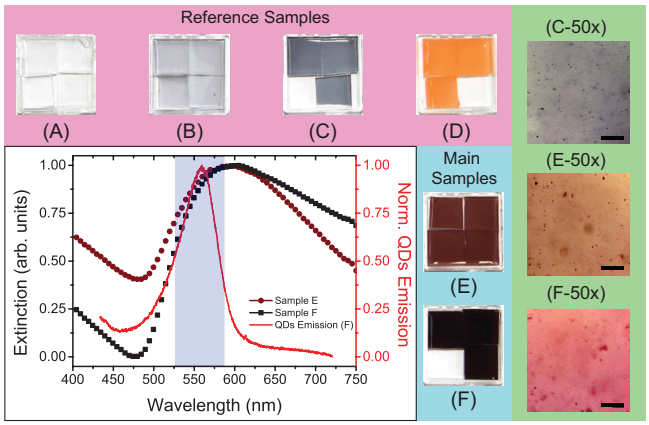

Fig. 1. Images of the reference and main samples. Reference samples (A) pure PDMS film, (B) low (1×10^{-6} M) and (C) high (3×10^{-6} M) concentrated Au-NPs PDMS film and (D) QDs-PDMS film (QDs concentration = 6×10^{-5} M). Main samples E and F: Dispersion of same concentration of QDs with low and high concentrated Au-NPs in PDMS matrix, respectively. Plasmon bands of samples E (brown circles) and F (black squares) and fluorescence emission spectrum of sample F (red line). Light blue background represents spectral overlapping region. Microscope images of sample C, E and F have been acquired by a 50x objective to show the uniform distribution of Au NPs and QDs aggregates of different size (C-50x, E-50x and F-50x). Scale bar measures 20μm.

3. Results and discussions

A multi-functional ultrafast experimental set-up has been utilized to study gain-plasmon interaction in plexcitonic systems, as shown in Fig. 2(a). Fluorescence quenching behavior of QDs in presence of Au-NPs and time resolved fluorescence spectroscopy have been performed in order to confirm their strong interaction. Samples D, E and F were pumped at excitation

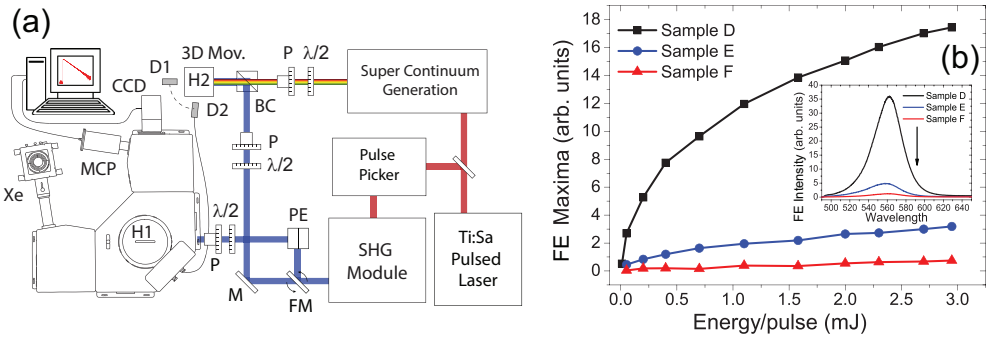

Fig. 2. (a) An ultrafast optical set-up designed for steady state fluorescence measures, time resolved spectroscopy and broadband pump-probe experiments. (b) Maxima of fluorescence emission (FE) intensity of sample E (blue circles) and sample F (red triangles) with respect to sample D (black squares) as a function of the incident pump energy. Inset shows the quenching of emission spectra of QDs in the presence of Au-NPs in sample E (blue line) and F (red line) with respect to sample D (black line).

wavelength $\lambda_{exc} = 370nm$ with same average power by a tunable (680-1080 nm range) femtosecond Ti:Sapphire pulsed laser (repetition rate = 4 MHz, pulse width = 140 fs, by Coherent

#261630 Received 22 Mar 2016; revised 9 May 2016; accepted 9 May 2016; published 21 Jun 2016

Inc.), coupled with a second harmonic generator (SHG) module, as shown in Fig. 2(a). Inset of Fig. 2(b) shows the fluorescence emission quenching of both sample E and F with respect to sample D. Fluorescence emission quenching in sample F have been observed more significant with respect to sample E, due to higher concentration of plasmonic nano-resonators. Moreover, observed emission quenching has also been reported as a signature of non-radiative energy transfer processes occurring from QDs to Au-NPs [25, 38]. In order to elucidate this point, the maxima of fluorescence emission intensity spectra of samples E and F are compared to sample (D) as a function of excitation energy. If QDs and Au-NPs are uncoupled, Au-NPs would act as a static quencher and quenching rate must be constant as a function of energy [28, 38]. Different rates have been instead observed for both hybrid samples, confirming that a non-radiative RET process is at the basis of the observed quenching mechanism [25, 28].

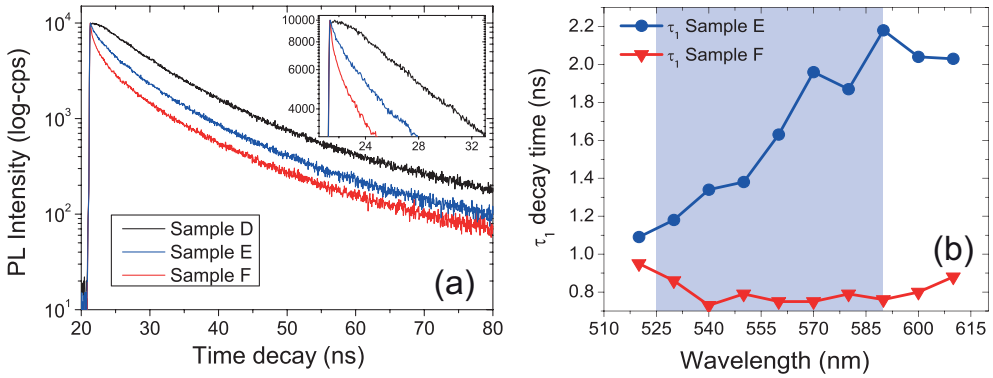

Fig. 3. (a) Time-resolved fluorescence intensity decays for sample D (black curve), sample E (blue) and F (red). Inset represents a zoom of the first 32 ns. (b) Shortened fast decay time τ_1 in sample F with respect to sample E at different emission wavelengths. Light blue background represents spectral overlapping region between plasmon bands of Au NPs and fluorescence emission of QDs.

Time-resolved fluorescence spectroscopy was carried out on samples E and F, as well as on reference sample D, in order to study the time dependent behavior behind the exciton-plasmon coupling and RET processes. Figure 3(a) shows time-resolved fluorescence intensity decays at fixed emission wavelength 560 nm, for main and reference samples, performed by means of a spectrofluorometer (by Edinburgh Inc.) excited at 370 nm by same frequency doubled pulsed laser described in Fig. 2. A bi-exponential fitting function is used to study the decay rate of QDs dispersed in PDMS, due to the formation of QDs micro-aggregates into the plastic matrix [32]. In the presence of Au-NPs, three exponential decay times were measured, including a very short decay time (τ_1). This very short living state is attributed to the fraction of QDs which is located in close proximity with Au-NPs and take part in *EPRET* process via strong gain-plasmon coupling. Appearance of τ_1 clearly shows that fluorescence emission quenching of

Table 1. Decay lifetime for sample D, E and F in ns at emission wavelength 560 nm.

Decay Time (ns)	Sample D	Sample E	Sample F
τ_1	–	1.96	0.75
τ_2	10.7	8.8	6.6
τ_3	45.6	38.5	28.5

QDs in the presence of Au-NPs is related to a faster relaxation dynamics, due to the presence of

#261630 Received 22 Mar 2016; revised 9 May 2016; accepted 9 May 2016; published 21 Jun 2016

a non-radiative channel, confirming a RET mechanism (see table 1 for details at emission wavelength of 560 nm). The intermediate lifetime (τ_2) is attributed to Förster-like resonance energy transfer (FRET-like) mechanism between the different sizes of QDs micro-aggregates [39, 40]. Life time τ_3 is originated from those agglomerated QDs which do not participate in any kind of energy transfer process. Moreover, we reported shortest life time components (τ_1) of sample E and F as a function of emission wavelength (see Fig. 3(b)). It is clearly evident that higher concentrated plexitonic elements (sample F) remain closer to each other with respect to lower concentrated ones, when dispersed in the identical host matrix. Faster non radiative energy transfer process from QDs to Au NPs via exciton-plasmon coupling strictly depends on exciton-plasmon inter-distance and spectral overlapping [38]. A large variation in τ_1 is observed in sample E due to weak plexcitonic coupling with respect to an almost constant behavior of sample F due to strong coupling as a function of emission wavelength, which becomes more pronounced inside spectral overlapping region as indicated by the light blue background of Fig. 3(b). It is interesting to mention here that similar constant behavior of life time as a function of emission wavelength has been observed in many other plasmon based nanostructures such as hyperbolic metamaterials, when excitons are strongly coupled to surface plasmon polariton modes of multilayer structures [41, 42]. An ultrafast broadband pump-probe experiment has been performed to measure simultaneously transmission and Rayleigh scattering of hybrid films under excitation wavelength $\lambda_{exc} = 400nm$. This represents the most important proof that EPRET processes are responsible of optical loss mitigation mechanism. Setup sketched in Fig. 2(a) allows the beam from a Ti:Sa pulsed laser to be split in two parts. 70% is duplicated by a SHG module (340 nm - 540 nm) representing the excitation beam. Remaining fraction of the

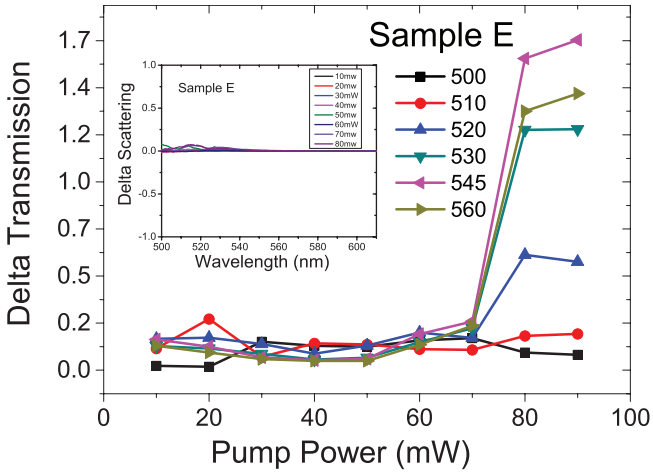

Fig. 4. Particular wavelength cuts extracted from broadband Δ_T of sample E in the spectral overlapping region of plasmon resonances and QDs emission as a function of pump power, when pumped by excitation wavelength $\lambda_{exc} = 400nm$. Inset shows the Delta scattering experiment as a function of spectral overlapping region wavelength for sample E.

beam is used to generate super continuum light from a nonlinear photonic crystal fiber, to obtain a broadband probe beam (500 – 1000 nm). Pump and probe beams are coupled by means of a beam coupler (BC) and sent to the sample holder. Here, we used 1 mm diameter probe beam placed in the central region of a 2 mm diameter of pump beam, which always allows to probe the area where maximum coupling between gain medium and plasmonic nanostructures is expected. This is due to the Gaussian intensity distribution of the two laser spots (pump and probe beams). Beer-Lambert-Bouguer law states that simultaneous investigations of a probe

#261630 Received 22 Mar 2016; revised 9 May 2016; accepted 9 May 2016; published 21 Jun 2016

beam in Rayleigh scattering and transmission measurements through pump-probe experiment allows us to understand whether gain is able to modify absorptive nature of plasmonic systems. Delta transmission Δ_T is defined as $(I_p - I_o)/I_o$, where I_p and I_o are the transmitted intensity of probe beam in the presence and in the absence of pump beam, while delta scattering Δ_S is defined in the same way, in terms of scattered probe beam. Figure 4 shows ultrafast pump-probe experiment for the simultaneous measure of transmission and Rayleigh scattering on sample E. Sample E shows transmission enhancement of probe beam for spectral overlapping wavelengths as a function of pump power. Weaker plexcitonic coupling present in such hybrid film enables gain induced transparency above a higher threshold value (above 70 mW) while the inset of Fig. 4 shows how the scattered probe beam is unaffected by the pump energy throughout the whole spectral overlapping region. It is evident from Fig. 5(a) how strong exciton-plasmon coupling takes place in the case of sample F. Δ_T remains constant at lower pump power and even demonstrates slight transmission enhancement at higher power for 500 nm probe wavelength which is just located at the edge of spectral overlapping region. On the contrary, Δ_T gradually increases as we change the wavelengths of the probe beam inside the spectral overlapping region as a function of pump power. Figure 5(a) reports lower threshold value (10 mW), above which a super linear enhancement of delta transmission through sample F has been observed. In fact, transmitted probe beam at 545 nm (90 mW pump power) is enhanced to an order of

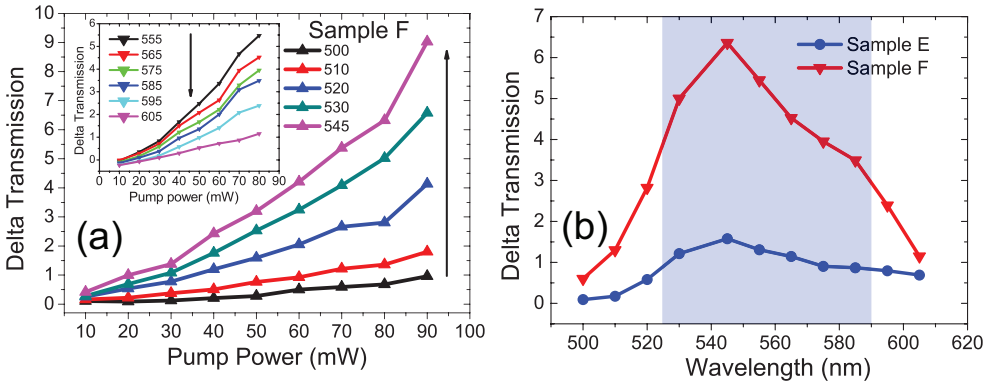

Fig. 5. (a) Particular wavelength cuts extracted from broadband Δ_T of sample F, approaching towards the maximum transparency, attained at 545 nm in the spectral overlapping region as a function of pump power. Inset shows decrease in Δ_T for sample F, when probe wavelengths move towards the end of overlapping region. (b) Comparison of Δ_T (pump power = 80 mW) for samples E and F as a function of probe wavelengths. Blue background represents the spectral overlapping region, evidencing the enhanced broadband optical transparency in sample F with respect to sample E.

magnitude with respect to one, obtained at 500 nm probe beam. Inset of Fig. 5(a) shows how Δ_T decreases when probe beam approach towards the end of overlapping region. Also in this case, Rayleigh scattering remains constant at all excitation powers (curves not reported here). Figure 5(b) shows behavior of delta transmission for sample E and F at a 80 mW pump power. Delta transmission enhancement, as well as observed threshold values, clearly highlight how effective EPRET processes are behind the induced broadband transparency obtained in sample F with respect to sample E. The decreasing of the large imaginary part of permittivity of such hybrid systems permits to attain a broadband mitigation of optical losses. In this context, Xiao et al. showed a transmitted probe beam enhancement of about 100%, within a wavelength range (712 to 736 nm), through gain functionalized plasmonic structures, by defining delta transmission in a similar way [43]. Even though the proposed structures are completely different from

#261630 Received 22 Mar 2016; revised 9 May 2016; accepted 9 May 2016; published 21 Jun 2016

our systems and cannot be compared to them, in terms of delta transmission we observed a net enhancement of probe beam through sample E and F in a wider wavelength region (520 - 600nm), with maximum values of about 150% and 650%, respectively, as reported in Fig. 5(b). Noteworthy, we performed the same pump probe experiments on all reference samples

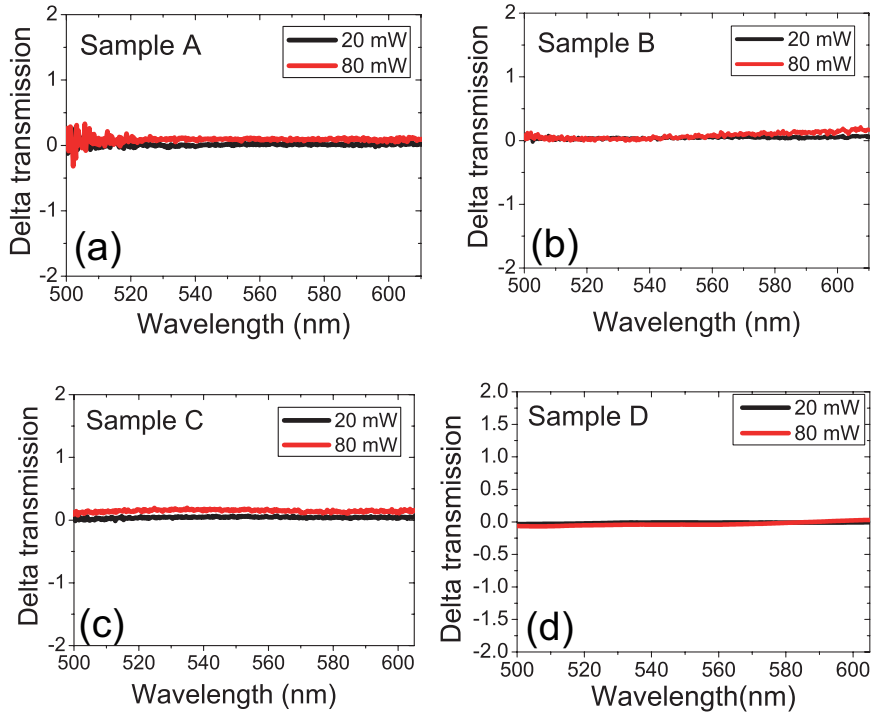

Fig. 6. Delta transmission (Δ_T) of reference samples for two extreme pump powers (20 mW & 80 mW) as the function of the spectral overlapping region(500-600 nm), when excited by excitation wavelength $\lambda_{exc} = 400nm$. (a) Sample A, (b) sample B, (c) sample C, (d) sample D. Black and red lines represent the responses of probe beam at 20 mW and 80 mW pump power, respectively.

A, B, C and D, inside the overlapping region and under the same experimental conditions as used in main samples (E & F). In this case we used only two extreme pump powers (20 mW & 80 mW). Figure 6 reports uniform and similar transmission signals at the two extreme pump values for all the wavelengths of the overlapping region (500-600nm). This ensures that only hybrid systems (sample E & F) exhibit transmission enhancement due to non-radiative energy transfer from QDs to Au NPs via exciton-plasmon coupling.

#261630 Received 22 Mar 2016; revised 9 May 2016; accepted 9 May 2016; published 21 Jun 2016

4. Conclusion

In summary, nanocomposite polymer films were fabricated by simultaneous dispersion of QDs and Au-NPs by properly acting on nanocrystals surface chemistry. We confirmed the presence of strong coupling mechanism between plexcitonic elements dispersed in a PDMS template and demonstrated how this coupling mechanism strongly modifies the optical response of the flexible films. Non radiative energy transfer processes from QDs to plasmonic NPs mitigates the absorptive losses and enables the entire system to be more transparent. In addition, presence of gain in close proximity of gold NPs was experimentally proved in order to achieve an efficient EPRET processes between excitons and plasmons in bulk matrix. Such hybrid films enable us to mimic more practical systems, where gain-plasmon concentrations can be controlled. Therefore we reported an example towards the realization of optical metamaterials based on gain functionalized plasmonic devices with low losses.

Acknowledgments

We acknowledge N. Depalo, E. Fanizza, M. L. Curri and M. Striccoli for first sample preparation and for the useful discussions. The research leading to these results has received support and funding from the Italian Project ”NanoLase” - PRIN 2012, Protocol No. 2012JHFYMC and from the Ohio Third Frontier Project Research Cluster on Surfaces in Advanced Materials (RC-SAM).

#261630 Received 22 Mar 2016; revised 9 May 2016; accepted 9 May 2016; published 21 Jun 2016